

Electron paramagnetic resonance studies on manganite $\text{Pr}_{0.5}\text{Sr}_{0.5}\text{Mn}_{1-x}\text{Ga}_x\text{O}_3$ ($x = 0$ and 0.05)

Jiyu Fan · Langsheng Ling · Bo Hong · Wei Tong · Lei Zhang · Yangguang Shi · Weichun Zhang · Yan Zhu · Dazhi Hu · Yao Ying · Li Pi · Yuheng Zhang

Received: 28 August 2012 / Accepted: 29 October 2012 / Published online: 18 November 2012
© Springer-Verlag Berlin Heidelberg 2012

Abstract In this paper, we present the investigations of electron paramagnetic resonance on perovskite manganite $\text{Pr}_{0.5}\text{Sr}_{0.5}\text{MnO}_3$ and Ga-doped $\text{Pr}_{0.5}\text{Sr}_{0.5}\text{Mn}_{0.95}\text{Ga}_{0.05}\text{O}_3$. The temperature dependent paramagnetic resonance spectra parameters (effective g -factor, peak-to-peak linewidth ΔH_{pp} and double integrated intensities) have been used to study the paramagnetic spin correlations and spin dynamics. The gradual increase of effective g -factor is attributed to the presence of orbital ordering above T_C . The model fittings of temperature dependent double integrated intensities reveal Arrhenius law is appropriate for describing $\text{Pr}_{0.5}\text{Sr}_{0.5}\text{Mn}_{0.95}\text{Ga}_{0.05}\text{O}_3$ instead of $\text{Pr}_{0.5}\text{Sr}_{0.5}\text{MnO}_3$ system. As for $\text{Pr}_{0.5}\text{Sr}_{0.5}\text{MnO}_3$, the broadening of linewidth with the temperature increase origins from the contribution of small polaron hopping in the PM regime. However, as for

$\text{Pr}_{0.5}\text{Sr}_{0.5}\text{Mn}_{0.95}\text{Ga}_{0.05}\text{O}_3$, the broadening of EPR linewidth can be understood with the spin-lattice relaxation mechanism.

1 Introduction

Electron paramagnetic resonance (EPR) is known as a powerful probe of spin dynamics and magnetic correlation in perovskite manganites on a microscopic level. By the analysis of temperature dependence of EPR spectra parameters (line shape, effective g -factor, peak-to-peak linewidth ΔH_{pp} , and double integrated intensities (DIN)), we can obtain many valuable information about spin dynamics and spin correlations. In this field, the discussion of the paramagnetic linewidth variation is always a hot issue [1–8]. Recently, Huber recalled in question the previous conclusion of the e_g polarons hopping contribution to EPR linewidth [9]. Therefore, it is well worth investigating the linewidth variation and the polarons hopping contribution to EPR linewidth.

Mixed-valence manganites with the general formula $\text{R}_{1-x}\text{A}_x\text{MnO}_3$ (R = rare earth element, A = divalent alkaline earth element) attracted great attention in recent years since that the basic physics of these materials is governed by the close interaction between lattice, spin, and charge degree of freedom [10–14]. Among these oxides, the half-doped manganites $\text{R}_{0.5}\text{A}_{0.5}\text{MnO}_3$ are particularly interesting, since they display the charge ordering (CO) which behaves like the periodic arrangement of $\text{Mn}^{3+}/\text{Mn}^{4+}$ ions associated with the magnetic order of either A-type antiferromagnetic (AFM) phase or CE-type (mixed magnetic structure of A- and C-type) AFM phase. The half-doped manganites $\text{Pr}_{0.5}\text{Sr}_{0.5}\text{MnO}_3$ is a typical CO material whose ground

J. Fan (✉) · Y. Shi · W. Zhang · Y. Zhu · D. Hu
Department of Applied Physics, Nanjing University
of Aeronautics and Astronautics, Nanjing 210016, China
e-mail: fanjiyu@gmail.com
Fax: +86-25-83336919

L. Ling · W. Tong · L. Zhang · L. Pi · Y. Zhang
High Magnetic Field Laboratory, Chinese Academy of Sciences,
Hefei 230031, China

B. Hong
Department of Material Engineering, China Jiliang University,
Hangzhou 310018, China

Y. Ying
Institute of Magnetic and Electronic Materials, College
of Chemical Engineering and Materials Science, Zhejiang
University of Technology, Hangzhou 310023, China

L. Pi · Y. Zhang
Hefei National Laboratory for Physical Sciences at the
Microscale, University of Science and Technology of China,
Hefei 230026, China

state is a A-type AFM phase and metallic layers with ferromagnetically ordered spins coupled antiferromagnetically to each other [15–17]. Even though its magnetism and CO character have been previously reported, the investigation of EPR on it is rarely performed.

In this paper, two samples of $\text{Pr}_{0.5}\text{Sr}_{0.5}\text{MnO}_3$ (PSMO) and Ga-doped $\text{Pr}_{0.5}\text{Sr}_{0.5}\text{Mn}_{0.95}\text{Ga}_{0.05}\text{O}_3$ (PSMGO) were studied. Through the substitution with Ga^{3+} ions, we can adjust/change the e_g polarons hopping in $\text{Pr}_{0.5}\text{Sr}_{0.5}\text{Mn}_{0.95}\text{Ga}_{0.05}\text{O}_3$ so that we can compare their contribution to paramagnetic (PM) linewidth with that of $\text{Pr}_{0.5}\text{Sr}_{0.5}\text{MnO}_3$. Our investigation indicates that for $\text{Pr}_{0.5}\text{Sr}_{0.5}\text{MnO}_3$ the broadening of linewidth and a linear temperature dependence of linewidth in the PM regime origin from the contribution of small polaron hopping. However, for $\text{Pr}_{0.5}\text{Sr}_{0.5}\text{Mn}_{0.95}\text{Ga}_{0.05}\text{O}_3$ the broadening of EPR linewidth with the temperature increase is due to the spin-lattice relaxation mechanism.

2 Experiment

Polycrystalline manganite $\text{Pr}_{0.5}\text{Sr}_{0.5}\text{Mn}_{1-x}\text{Ga}_x\text{O}_3$ ($x = 0$ and 0.05) samples were prepared by the conventional solid-state reaction method described in [18]. The dc magnetic susceptibility was measured by using a commercial superconducting quantum interference device magnetometer (Quantum Design MPMS 7T-XL) and the resistivity (ρ) was measured by standard four-probe method. The EPR measurement of the powder sample was performed at selected temperatures using a Bruker EMX-plus model spectrometer with a heater operating at X-band frequencies ($\nu \approx 9.4$ GHz).

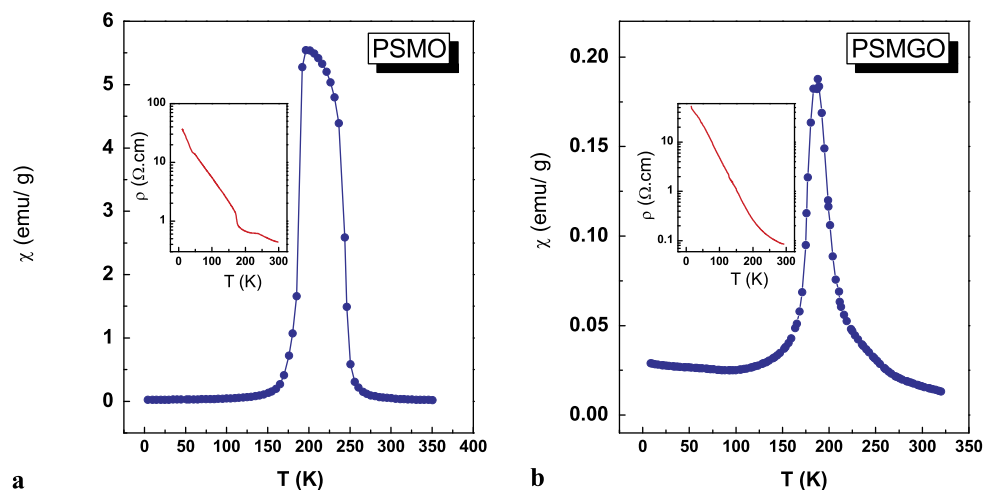
3 Results and discussion

The temperature variation of the dc magnetic susceptibility was shown in Fig. 1. As for PSMO sample, the susceptibility

curve shows a sharp PM–FM transition at ~ 250 K and then turns to ferromagnetic (FM)–AFM transition at ~ 200 K. Obviously, the FM–AFM transition is associated with the formation of charge ordering phase at $T = 200$ K. The inset of Fig. 1(a) shows the temperature dependence of resistivity ($\rho \sim T$) curves. As for a strong correlated magnetic transport system, its electronic transport behavior is closely related to its magnetic properties. Therefore, upon cooling from 200 K, the rapid increase of resistivity just corresponds to the decrease of susceptibility in Fig. 1(a) due to the FM–AFM transition. These observed results are in agreement with the previous reports in the same materials [19, 20], indicating that the present sample is high quality. As for PSMGO sample, its properties of magnetic susceptibility and electronic transport are similar to that of PSMO sample due to the low dopant content (5 wt%) adopted in the current sample. However, as shown in inset of Fig. 1(b), it has been impossible to observe an obvious charge ordering transition from its $\rho \sim T$ curve implying that the parent spin–orbital coupling has been changed the Ga-substitution.

Let us now study the experimental EPR data of PSMO and PSMGO samples. Both of them appear that all EPR lines are a single Lorentzian at temperature above that of magnetic phase transition (not shown here). Upon cooling, the resonance field gradually moves to the low field regime, corresponding to that of FM phase transition in Fig. 1. With further cooling, the resonance lines not only broaden but also the EPR line deviates from Lorentzian shape and exhibits a large distortion. Here, in order to penetrate into the change of EPR line, Fig. 2 gives the g value as a function of temperature. The g value can be calculated from the resonance field formula $g = h\nu/\mu_B H_{\text{res}}$ (h is the Plank constant; ν is the frequency of the microwave; μ_B is the Bohr magneton). Generally, the EPR signal in manganites has been attributed to the contribution from Mn^{4+} rather than Mn^{3+} ions, because Mn^{4+} ions have an isotropic g value of ~ 1.99 in an octahedral crystal field while Mn^{3+}

Fig. 1 The temperature dependence of the dc magnetic susceptibility; the inset shows the temperature variation of the measured electrical resistivity



ions have large zero-field splitting and very short spin-lattice relaxation time [21]. As for PSMO sample, the calculated g value increases from 2.14 to 2.37 as the temperature decreases from 300 to 250 K. In the PM regime, however, the g value should remain unchanged. Therefore, the increase of g value here implies that an additional spin correlation occurs in PSMO sample above the temperature of PM–FM phase transition. One similar increase of g value was also previously reported in the $\text{Nd}_{0.5}\text{Sr}_{0.5}\text{MnO}_3$ [3]. From 250 to 220 K, the g value shows a prominent increase indicating the development of orbital ordering. The above increase in g value can be understood from the changes in the spin–orbit coupling constant consequent to the orbital ordering which can influence the crystal field splitting and hence can lead to an increase in the g value. As for PSMGO sample, however, the g value decreases from 2.29 to 2.20 as the temperature changes from 300 to 240 K. Moreover, the g value exhibits a noticeable decrease as $T < 240$ K and reaches to 1.86 at $T = 180$ K. Therefore, the Ga dopant not only changes the parent spin correlation in the PM regime but also suppresses the development of orbital ordering.

In the following section, we discuss the temperature dependence of the EPR linewidth ΔH_{pp} which is defined as the width between the highest point and the lowest one in the EPR spectrum. As shown in Fig. 3, the ΔH_{pp} curves

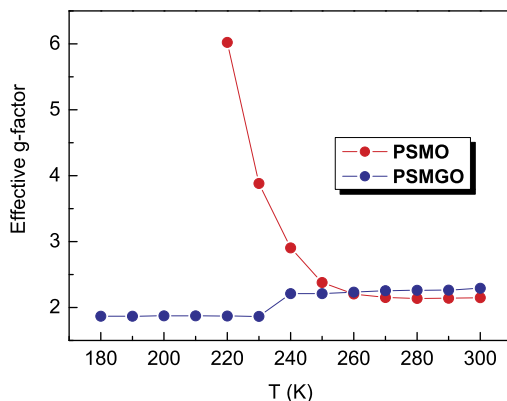
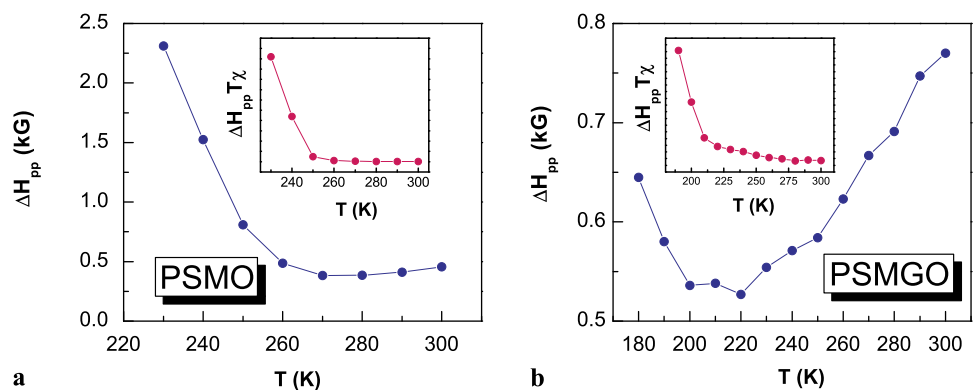


Fig. 2 The effective g -factor as a function of temperature

Fig. 3 The EPR linewidth ΔH_{pp} versus T (the inset plots the temperature dependence of the product $\Delta H_{\text{pp}}T\chi$)



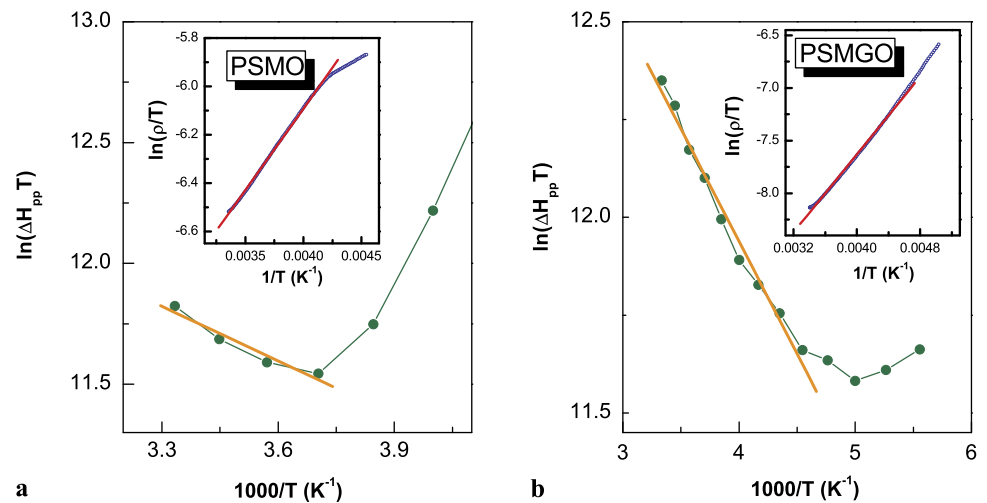
of both samples exhibit minimum values at temperatures called T_{min} . Their T_{min} are 270 and 220 K, respectively. Such a feature is common in manganites. Through comparing the ΔH_{pp} variation in Fig. 3(a) with that in Fig. 3(b), one can find that the PSMGO sample exhibits one more obvious broadening of ΔH_{pp} . In the PM regime, the broadening of the EPR linewidth arises from shortening of spin–lattice relaxation time due to the hopping of e_g electrons via spin–orbit coupling. As Ga ions occupy the Mn^{3+} positions, the parent lattice structure inevitably changes. From the above studies of the g value, the spin correlation has been confirmed in the PM regime. Therefore, the variation of lattice structure necessarily affects the spin–lattice coupling and decreases the spin–lattice relaxation time. Thus, a larger broadening of ΔH_{pp} was observed in the Ga-doped PSMGO sample. In the PM regime, the linewidth can be described by the expression [1]:

$$\Delta H_{\text{pp}}(T) = \Delta H_{\text{pp}}(\infty) \frac{C}{T\chi} \quad (1)$$

where C/T is the single ion susceptibility, χ is the measured paramagnetic susceptibility, and $\Delta H_{\text{pp}}(\infty)$ is the linewidth expected at a high enough temperature. The above formula can be rewritten as $\Delta H_{\text{pp}}(T)T\chi = \Delta H_{\text{pp}}(\infty)C$. As there are no spin–phonon interactions in the PM regime, the product $\Delta H_{\text{pp}}T\chi$ should be a temperature independent constant. The insets of Figs. 3(a) and 3(b) show the product $\Delta H_{\text{pp}}T\chi$ as a function of temperature above T_C . Both of them show a slight increase with the decrease of temperature, indicating that there exists a contribution of spin–phonon interactions to the linewidth ΔH_{pp} variation. Moreover, the inset of Fig. 3(b) shows a more significant increase. Therefore, the spin–phonon interactions are more sensitive to temperature changes in the PSMGO sample because the Ga substitution changes the vibrations of the lattice.

For the most of hole-doped manganites, the electronic transport behavior is generally considered to be polaron hopping in the PM regime. Therefore, the contribution of the polarons hopping to EPR linewidth is worth investigating. However, up to now, the question has not been com-

Fig. 4 EPR linewidth plotted as $\ln(\Delta H_{pp}T)$ vs $1000/T$ (the solid line represents the fitting results of (2)); the inset plots $\ln(\rho/T)$ versus $1/T$ and the solid line are fits to the small polaron hopping model



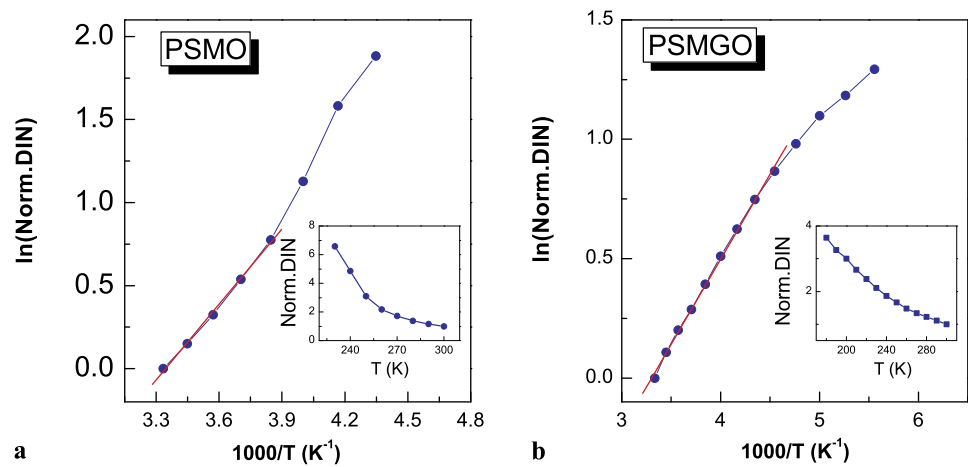
pletely solved. The issue was first brought up by Shengelaya et al. in the investigation of $\text{La}_{1-x}\text{Ca}_x\text{MnO}_3$, and they proposed a “bottleneck model” to describe the temperature dependence of the EPR linewidth ΔH_{pp} [21]. In order to clarify the polaron contribution, Huber et al. provided another theoretical formula which could characterize the EPR linewidth in the absence of polaron contribution [22]. However, in subsequent investigation of $\text{Pr}_{0.8}\text{Ca}_{0.2}\text{MnO}_3$ [24] and $\text{La}_{0.75}\text{Ca}_{0.25}\text{MnO}_3$ [23], irrespective of whether one considers the polaron contribution or not, both models gave nearly identical fitting results. Therefore, it is difficult to affirm the contribution of polaron hopping to the EPR linewidth. Beyond that, other models, such as one-phonon process [25] and a spin-only relaxation mechanism [1], are also used to explain the EPR linewidth variation in the PM regime. In the present system, the hopping of e_g electrons from Mn^{3+} to Mn^{4+} via the neighboring O^{2-} ions will determine the lifetime of the spin state and the EPR linewidth. The Ga-dopants aggravate the lattice distortion which will cause localization of carriers. Thus, we can directly obtain some information about the contribution of polaron hopping by comparing their activation energy obtained from the $\rho \sim T$ and $\Delta H_{pp} \sim T$ curves. Based on a small polaron model ($\rho = AT \exp(E_0/k_B T)$) and the $\rho \sim T$ curves of the inset of Fig. 1, the fitting curves are shown in the inset of Fig. 4. The obtained activation energy E_0 was deduced to be 58.1 meV for PSMO and 75.6 meV for PSMGO, respectively. Obviously, a larger activation energy in the PSMGO sample is entirely reasonable due to the Ga dopant assistance for carrier localization and the increase of activation energy. Now, we turn to deducing the activation energy variation from $\Delta H_{pp} \sim T$ curves. According to the “bottleneck model” [21], the activation energy can be deduced by using the following equation:

$$\Delta H_{pp}(T) = \Delta H_0 + \frac{A}{T} \exp(-E_a/k_B T) \quad (2)$$

where ΔH_0 and A are two temperature-independent parameters and E_a is the activation energy. Figure 4 shows the $\ln(\Delta H_{pp}T)$ versus $1000/T$, and the straight line represents the fitting results. The activation energy E_a is 64.8 meV for PSMO and 49.6 meV for PSMGO, respectively. Comparing the obtained activation energy from two different approaches, we can find that the values of the PSMO sample are in a reasonable range of error while the values of PSMGO have a relatively large deviation. As for the activation energy obtained from the $\rho \sim T$ curves, we should admit its reliability because it was deduced directly from the experimental electronic transport measurements. Assuming this to be the case, the presence of inconformity signifies that the polaron hopping contribution to linewidth variation is unsuitable for the Ga-doped PSMGO sample. A plausible interpretation of the deviation is that the Ga dopant causes an inhomogeneous magnetic domain distribution or a magnetic frustration, where the co-presence of PM, FM, and AFM interactions influences the spin–lattice relaxation. As a result, the detected linewidth variation is not consistent with the polaron hopping model.

In order to further clarify the issue, we studied the intensity variation of the EPR spectra which was an important parameter to identify the magnetic ions contribution to the resonant entities. Generally, one can use two different numerical analysis methods to investigate the intensity of the EPR spectra. The first one is the double integration of the spectra (dP/dH), and the second one is the calculation of the area of production $\Delta H_{pp}^2 Y'$ ($2Y'$ is the peak-to-peak derivative amplitude). However, the double integrated intensities (DIN) provided better accuracy for absolute values. Therefore, we here use the DIN to study the intensity of the EPR spectra. The intensity of the EPR spectra is associated with the total magnetic ions contribution to the resonant spectra. Therefore, in order to facilitate the numerical analysis, the DIN values are generally normalized to high temperature

Fig. 5 Arrhenius plots of DIN and the solid line represent the fitting results of (3) (the inset represents temperature dependence of the double integrated intensity DIN)



DIN ones. The inset of Fig. 5 shows the results of normalized DIN. Both figures show that the DIN values increase with the decrease of temperature. In the PM regime, the DIN for many manganites is usually described by the Arrhenius law [1, 26]:

$$\text{DIN}(T) = I_0 \exp(E_a/k_B T) \quad (3)$$

where E_a is the activation energy for dissociation of the paramagnetic spin clusters. As shown in Fig. 5, the activation energy was deduced to be 130 meV for PSMO and 61.4 meV for PSMGO, respectively. Obviously, for the PSMO sample, the too large activation energy of 130 meV indicates that the scenario of dissociation of the paramagnetic spin clusters cannot be applied to the PM regime of the PSMO sample. On the contrary, the dissociation of the paramagnetic spin clusters is very appropriate for the PSMGO sample since the Ga-dopant separates the $\text{Mn}^{3+}-\text{O}^{2-}-\text{Mn}^{4+}$ spin chain structure. In view of semiconducting transport in its PM regime, we also attempted using the thermal activation model ($\rho = \rho_0 \exp(E_P/k_B T)$) to fit the $\rho \sim T$ curve of Fig. 1(b). Unexpectedly, the obtained thermal activation energy E_P is 61.75 meV, which is strikingly similar to the value of $E_a = 61.4$ meV deduced from the DIN curve, indicating that the broadening of the EPR linewidth in PSMGO is not due to the polaron hopping mechanism. Namely, the description of electronic transport of PSMGO is better with the thermal activation model than with the small polaron model. Therefore, for the PSMGO sample, we think that the broadening of ΔH_{pp} with increasing temperature is associated with the spin lattice relaxation involving the one phonon process. In this doped system, the increase of temperature can assist the thermal motion of the lattice, which benefits the energy exchange among the different spin clusters. Thus, it causes the decrease of spin–lattice relaxation time and the increase of the EPR linewidth.

4 Conclusion

In summary, we have measured the dc magnetic susceptibility, electronic transport, and the EPR spectra for the ceramic $\text{Pr}_{0.5}\text{Sr}_{0.5}\text{MnO}_3$ and $\text{Pr}_{0.5}\text{Sr}_{0.5}\text{Mn}_{0.95}\text{Ga}_{0.05}\text{O}_3$. Together with the analysis of the effective g value, linewidth variation, and DIN, we found that the broadening of linewidth and a linear temperature dependence of linewidth in the PM regime arose from the contribution of small polaron hopping for $\text{Pr}_{0.5}\text{Sr}_{0.5}\text{MnO}_3$. However, for Ga-doped $\text{Pr}_{0.5}\text{Sr}_{0.5}\text{Mn}_{0.95}\text{Ga}_{0.05}\text{O}_3$, the broadening of the EPR linewidth with the increase of temperature stems from the spin–lattice relaxation mechanism.

Acknowledgements This work was supported by the National Nature Science Foundation of China (Grant Nos. 10904149, 11004196, 10334090, 11204131, 11204270, 51202235 and 51001061).

References

1. M.T. Causa, M. Tovar, A. Caneiro, F. Prado, G. Ibañez, C.A. Ramos, A. Butera, B. Alascio, X. Obradors, S. Piñol, F. Rivadulla, C. Vázquez-Vázquez, M.A. López-Quintela, J. Rivas, Y. Tokura, S.B. Oseroff, *Phys. Rev. B* **58**, 3233 (1998)
2. M.S. Seehra, M.M. Ibrahim, V.S. Babu, G. Srinivasan, *J. Phys. Condens. Matter* **8**, 11283 (1996)
3. S. Angappane, M. Pattabiraman, G. Rangarajan, K. Sethupathi, V.S. Sastry, *Phys. Rev. B* **69**, 094437 (2004)
4. S. Angappane, M. Pattabiraman, G. Rangarajan, K. Sethupathi, *J. Appl. Phys.* **97**, 10H705 (2005)
5. A.I. Shames, E. Rozenberg, G. Gorodetsky, Ya.M. Mukovskii, *Phys. Rev. B* **68**, 174402 (2003)
6. E. Rozenberg, M. Auslender, A.I. Shames, Ya.M. Mukovskii, E. Sominski, A. Gedanken, *J. Appl. Phys.* **105**, 07D707 (2009)
7. E. Rozenberg, A.I. Shames, M.I. Tsindlekht, I. Felner, Ya.M. Mukovskii, *J. Appl. Phys.* **111**, 07D702 (2012)
8. J. Fan, W. Tong, L. Zhang, Y. Shi, Y. Zhu, D. Hu, W. Zhang, Y. Ying, L. Ling, L. Pi, Y. Zhang, *Phys. Status Solidi B* **249**, 1634 (2012)
9. D.L. Huber, *J. Magn. Magn. Mater.* **324**, 2113 (2012)
10. R. von Helmolt, J. Wecker, B. Holzapfel, L. Schultz, K. Samwer, *Phys. Rev. Lett.* **71**, 2331 (1993)

11. S. Jin, T.H. Tiefel, M. McCormack, R.A. Fastnacht, R. Ramesh, L.H. Chen, *Science* **264**, 413 (1994)
12. K. Chahara, T. Ohno, M. Kassai, Y. Kozono, *Appl. Phys. Lett.* **63**, 1990 (1993)
13. A. Moreo, S. Yunoki, E. Dagotto, *Science* **283**, 2034 (1999)
14. M. Tokunaga, N. Miura, Y. Tomioka, Y. Tokura, *Phys. Rev.* **57**, 5259 (1998)
15. H. Kawano, R. Kajimoto, H. Yoshizawa, Y. Tomioka, H. Kuwahara, Y. Tokura, *Phys. Rev. Lett.* **78**, 4253 (1997)
16. F. Damay, C. Martin, M. Hervieu, A. Maignan, B. Raveau, *J. Magn. Magn. Mater.* **184**, 71 (1998)
17. Y. Tomioka, A. Asamitsu, Y. Moritomo, H. Kuwahara, Y. Tokura, *Phys. Rev. Lett.* **74**, 5108 (1995)
18. J. Fan, L. Ling, B. Hong, L. Zhang, L. Pi, Y. Zhang, *Phys. Rev. B* **81**, 144426 (2010)
19. K. Knizek, Z. Jirak, E. Pollert, F. Zounova, *J. Solid State Chem.* **100**, 292 (1992)
20. J.H. Jung, H.J. Lee, T.W. Noh, E.J. Choi, Y. Moritomo, Y.J. Wang, X. Wei, *Phys. Rev. B* **62**, 481 (2000)
21. A. Shengelaya, G.-m. Zhao, H. Keller, K.A. Müller, *Phys. Rev. Lett.* **77**, 5296 (1996)
22. D.L. Huber, G. Alejandro, A. Caneiro, M.T. Causa, F. Prado, M. Tovar, S.B. Oseroff, *Phys. Rev. B* **60**, 12155 (1999)
23. D.L. Huber, D. Laura-Ccahuana, M. Tovar, M.T. Causa, *J. Magn. Magn. Mater.* **310**, e604 (2007)
24. V. Markovich, I. Fita, A.I. Shames, R. Puzniak, E. Rozenberg, C. Martin, A. Wisniewski, Y. Yuzhelevskii, A. Wahl, G. Gorodetsky, *Phys. Rev. B* **68**, 094428 (2003)
25. C. Rettori, D. Rao, J. Singley, D. Kidwell, S.B. Oseroff, M.T. Causa, J.J. Neumeier, K.J. McClellan, S.-W. Cheong, S. Schultz, *Phys. Rev. B* **55**, 3083 (1997)
26. A.I. Shames, E. Rozenberg, W.H. McCarroll, M. Greenblatt, G. Gorodetsky, *Phys. Rev. B* **64**, 172401 (2001)